



Department of Computer Science

Color Uniformity and Moire in Dispersed Dot Halftone Masks Generated by Linear Pixel Shuffling

Peter G. Anderson Jonathan S. Arney Mark S. Guittard
Rochester Institute of Technology, Rochester, NY, USA

March 25, 2002

Abstract

Investigate a method for combining two dispersed-dot halftoning masks for two colors that generalizes the traditional angular displacement used with clustered-dot halftone screens.



What Are the Masks?

We used two variations of the Linear Pixel Shuffling algebraic mask algorithm involving numbers arising from two third order, Fibonacci-like recurrences,

As an alternative to screen rotation, masks were flipped and rotated.

All combinations of the transposed, inverted masks were used to generate 25% cyan and 25% magenta images.

Resulting blue images were evaluated for color uniformity several ways.



Background: Dispersed Dot Halftoning Masks

Quantize gray-scale image, I , to bi-level image, B , with a mask, M :

$$B_{pq} = \begin{cases} 1, & \text{if } I_{pq} \geq M_{pq} \\ 0, & \text{if } I_{pq} < M_{pq} \end{cases}$$

Mask & image values are in the same range: 0–255 or 0.0–1.0.

M can be constructed many ways:

Roberts's method uses pseudorandom numbers (white noise) and produces barely acceptable, mottled, bi-level images.

B. Bayer's method uses M in terms of replicated sub-windows or tiles.



Third-Order Sequences \mathcal{G} and \mathcal{T}

$$G_0 = 0, \quad G_1 = G_2 = 1 \quad G_n = G_{n-1} + G_{n-3} \text{ for } n > 2$$

$$T_0 = 0, \quad T_1 = T_2 = 1 \quad T_n = T_{n-1} + T_{n-2} + T_{n-3} \text{ for } n > 2$$

(\mathcal{T} is the **Tribonacci sequence**.)

Algebraic Masks

Let $A = S_n$, $B = S_{n+1}$, $C = S_{n+2}$, where S is \mathcal{G} or \mathcal{T} .

Define M by the rule $M_{pq} = (pA + qB) \% C$.

M is periodic in p and q with period C ,

M is a $C \times C$ tile of values $\{0, 1, \dots, C - 1\}$, each appearing C times.

(A consequence of $\gcd(S_n, S_{n+1}, S_{n+2}) = 1$ for both sequences.)

Why Use Algebraic Masks?

These masks are particularly convenient.

Each value can be computed from the value to its left or above by addition and a conditional subtraction—the table does not need to be stored.

The noise characteristics of the quantized images are good.

Algebraic Mask: $M_{pq} = (6p + 9q) \% 13$

0	9	5	1	10	6	2	11	7	3	12	8	4
6	2	11	7	3	12	8	4	0	9	5	1	10
12	8	4	0	9	5	1	10	6	2	11	7	3
5	1	10	6	2	11	7	3	12	8	4	0	9
11	7	3	12	8	4	0	9	5	1	10	6	2
4	0	9	5	1	10	6	2	11	7	3	12	8
10	6	2	11	7	3	12	8	4	0	9	5	1
3	12	8	4	0	9	5	1	10	6	2	11	7
9	5	1	10	6	2	11	7	3	12	8	4	0
2	11	7	3	12	8	4	0	9	5	1	10	6
8	4	0	9	5	1	10	6	2	11	7	3	12
1	10	6	2	11	7	3	12	8	4	0	9	5
7	3	12	8	4	0	9	5	1	10	6	2	11

Quantized Image with $A=81$, $B=149$, $C=274$



Problem: Masks for Multiple Color Planes

To avoid moire, printers rotate color planes relative to each other.

This rotation also achieves an independence of two colors, A and B , relative to each other.

The area fraction of color A overlapping color B is the area fraction of color A by itself. And vice versa.

This avoids inadvertent color shifting from two extremes: printing A on top of B , or color A completely missing color B .



Problem: Masks for Multiple Color Planes

How can we generalize algebraic masks to color printing to achieve what traditional printers achieve with rotated clustered dots patterns?

Experiments With Pairs of Algebraic Masks

Rotating a digital mask is difficult.

So, we create different masks by reflection and 90° rotations.

Eight symmetries are possible.



Symmetry Nomenclature for the \mathcal{G} Masks

G_0	\mathcal{G} mask in standard position
G_1	G_0 rotated 90° counter-clockwise
G_2	G_0 rotated 180° counter-clockwise
G_3	G_0 rotated 270° counter-clockwise
G_4	G_0 flipped top to bottom
G_5	G_4 rotated 90° counter-clockwise
G_6	G_4 rotated 180° counter-clockwise
G_7	G_4 rotated 270° counter-clockwise

Mask Specifics

T_0 mask parameters: $A = 274$, $B = 504$, $C = 927$.

G_0 mask parameters: $A = 595$, $B = 872$, $C = 1278$.

Images are 25% cyan, 25% magenta.

Use $7 + 7 + 8 = 22$ pairs of masks, as follows:

$$\langle G_0, G_1 \rangle, \quad \dots, \quad \langle G_0, G_7 \rangle$$

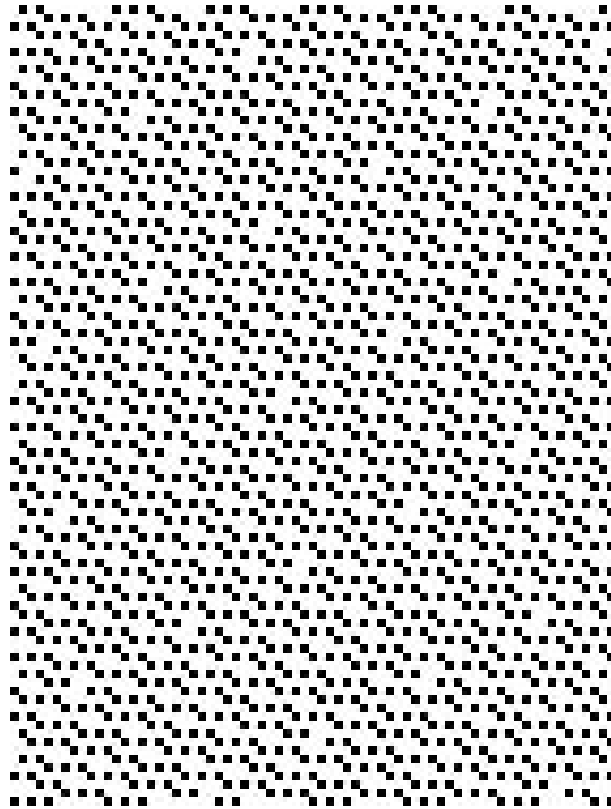
$$\langle T_0, T_1 \rangle, \quad \dots, \quad \langle T_0, T_7 \rangle$$

$$\langle G_0, T_0 \rangle, \quad \dots, \quad \langle G_0, T_7 \rangle$$

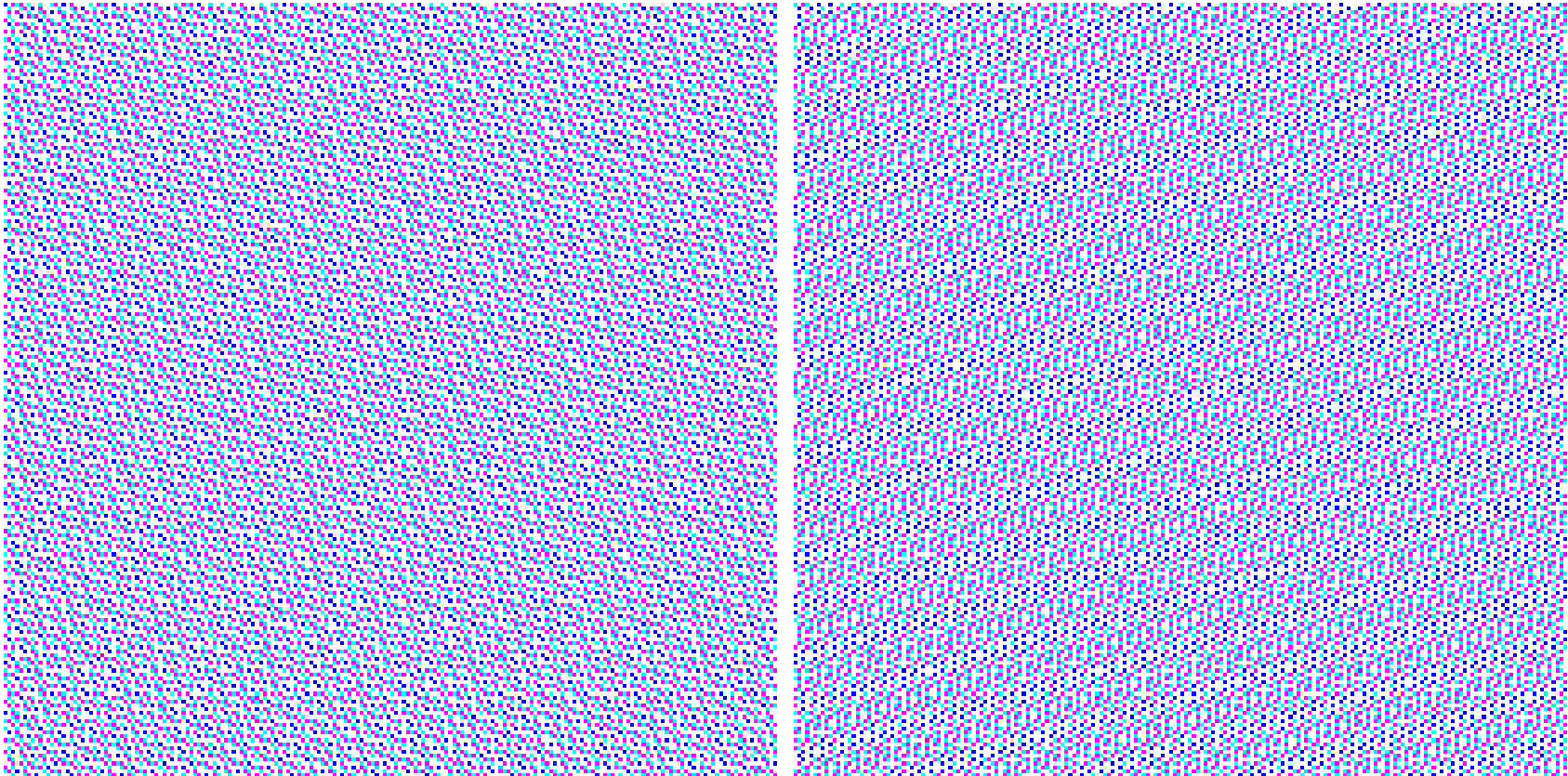
$\langle M, M' \rangle$ means M quantizes cyan and M' quantizes magenta.



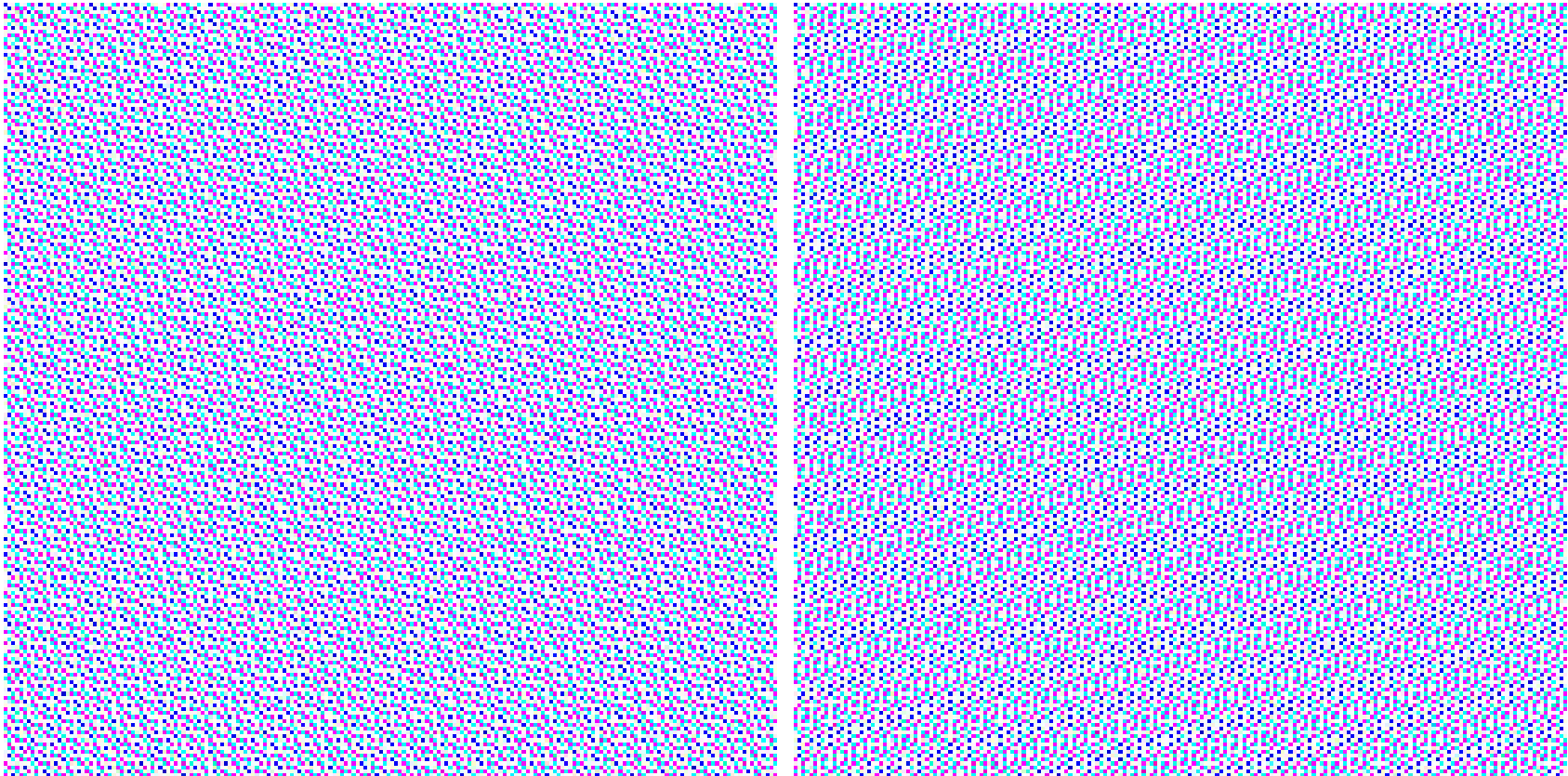
25% Gray Tribonacci Quantized—Params: 81, 149, 274



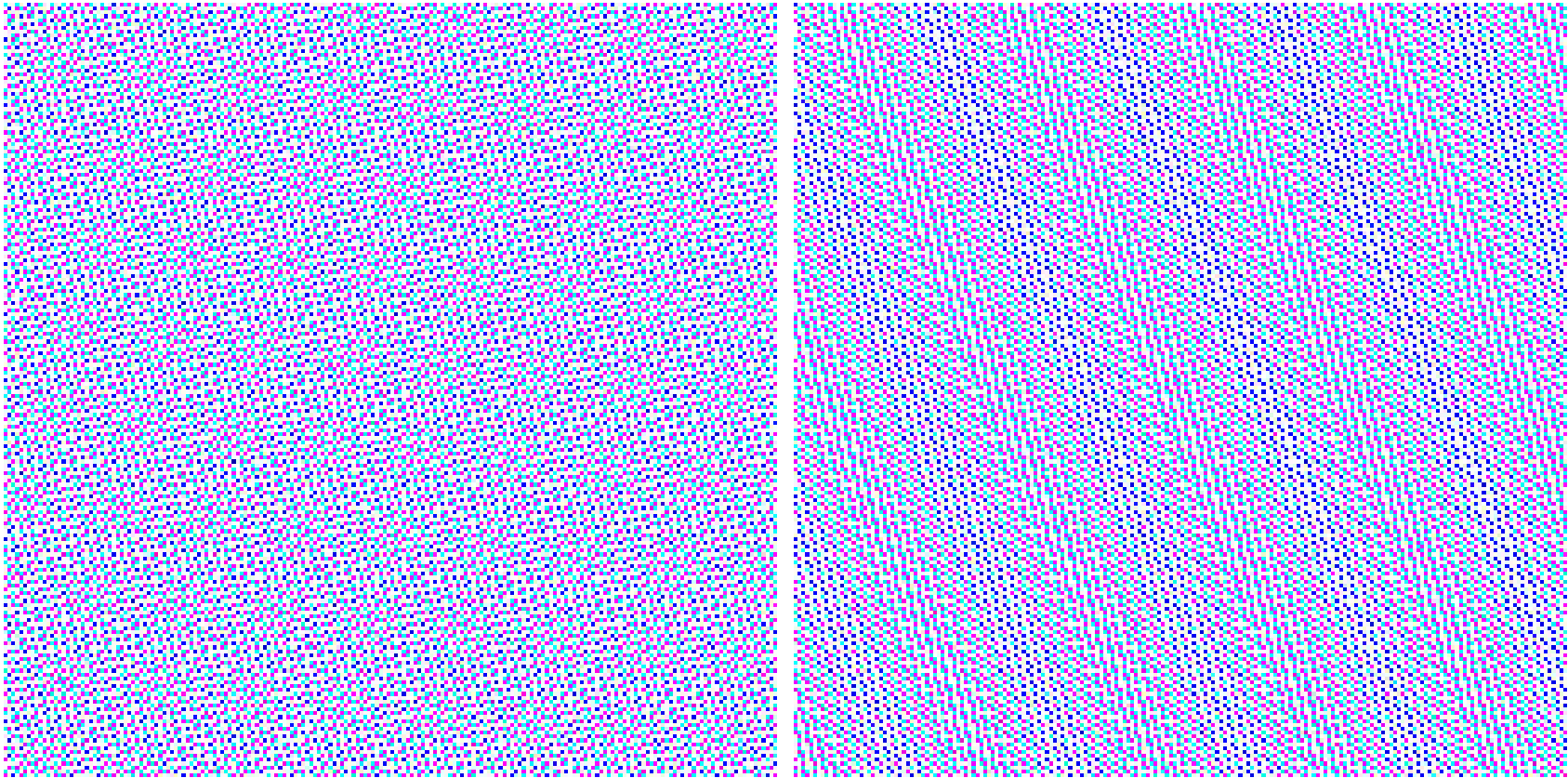
$$\langle G_0, T_0 \rangle, \langle G_0, T_1 \rangle$$



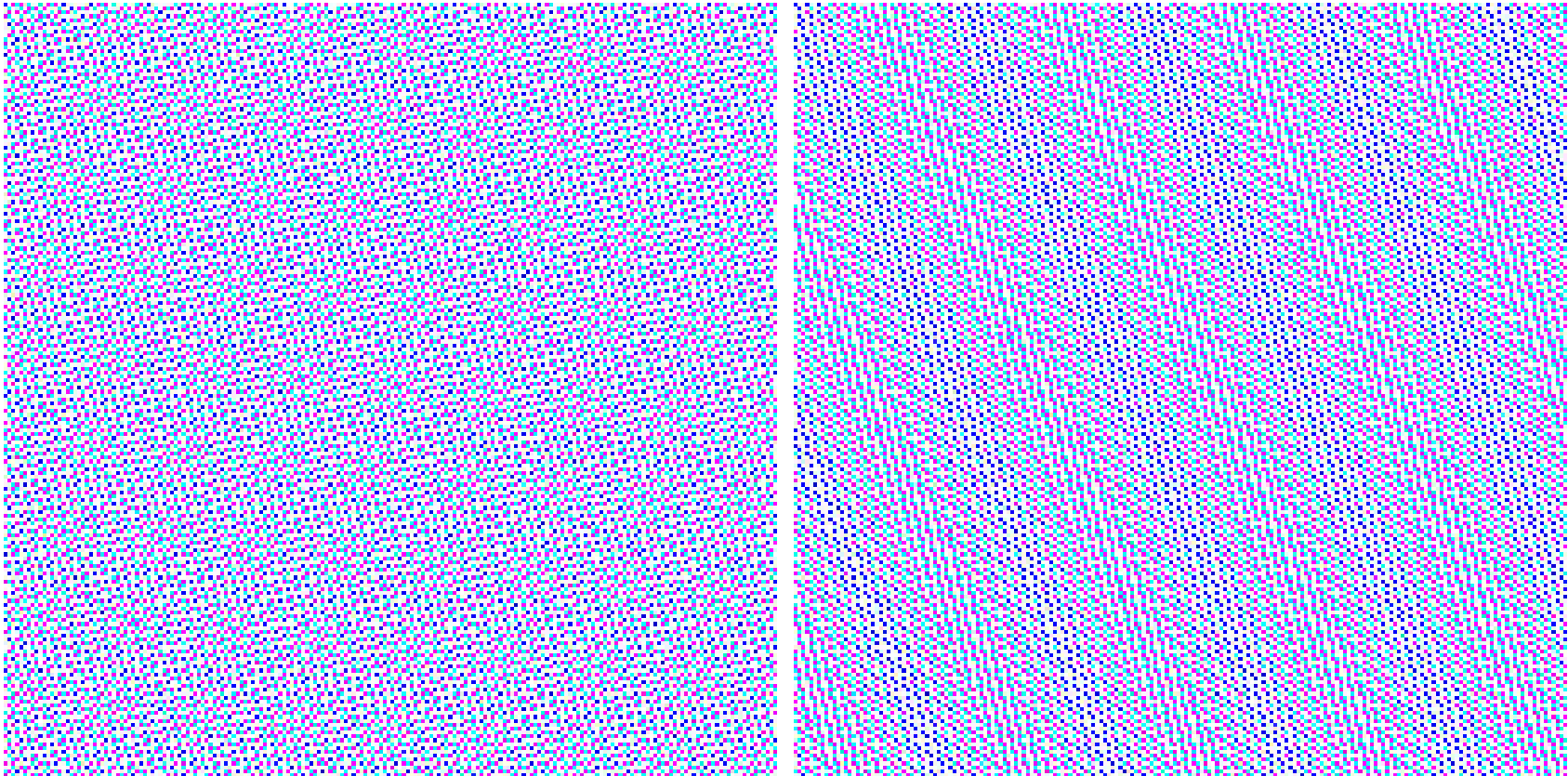
$$\langle G_0, T_2 \rangle, \langle G_0, T_3 \rangle$$



$$\langle G_0, T_4 \rangle, \langle G_0, T_5 \rangle$$



$$\langle G_0, T_6 \rangle, \langle G_0, T_7 \rangle$$



22 Color Images Were Evaluated With 3 Methods

1. Visual assessment of color uniformity.
2. Frequency composition (Fourier) analysis.
3. Box analysis to study the variation of the image in sampled sub-windows.

(We used the J programming language to generate the images. The results are summarized in the table below.)

Visual Assessment: Forming Computer Screen Images

Blue halftone images were simulated on a color CRT monitor by using cyan masks to control the red phosphors and magenta masks to control the green phosphors.

The blue was always at 100% output.

The simulated halftone dots were constructed as 1 mm. \times 1 mm. dots. With a monitor screen resolution of six RGB dots per millimeter, the simulated halftone dots contained approximately 36 phosphor dots.

Halftone dots representing cyan ink were displayed with the blue and green phosphors at 100% output and the red phosphor at 0% output. Similarly, the magenta halftone dots used red and blue phosphors with the green turned off. Blue dots were formed with the blue phosphor only.



Visual Assessment of Blue (B+C+M+W) Halftones

The relative spatial uniformity of the simulated blue halftones were evaluated visually.

Each blue halftone was displayed individually on the monitor.

We could easily see the individual 1 mm. \times 1 mm. dots of C, M, B, & W at a distance of 0.5 meter.

We increased the viewing distance until all four colors blended to a uniform blue.

The relative quality of the mask combinations was the metric of relative color uniformity.

Results are shown in the second column of the Metrics Table.



Fourier Analysis — Noise Power Analysis

A noise power analysis was also applied to the blue halftone images as a means of estimating the relative spatial uniformity of the 22 mask combinations.

In this case the simulated halftone image was constructed within the computer by defining reflection spectra for the virtual paper ($R_p = 1.00$ for 400–700 nm); for the virtual cyan ink ($R_c = 0.00$ for 600–700 nm and 1.00 elsewhere); and for the virtual magenta ink ($R_m = 0.004$ for 500–600 nm and 1.00 elsewhere).

The reflectance of the overlap blue was defined as 1.00 from 500 to 700 nm, and zero elsewhere. Each of the 22 mask combinations produced an array of colored dots of cyan, magenta, blue, and white. The $L^*a^*b^*$ value



for each pixel was calculated from the defined reflection spectrum of each pixel. The average reflectance spectrum for the image was calculated and the corresponding $L^*a^*b^*$ for the overall image determined.

A color difference, ΔE , between the halftone dot and the overall image was calculated for each individual dot. The resulting matrix of ΔE values was a spatial distribution of color variation for the blue halftone.

A variation matrix of this kind was determined for each of the 22 mask combinations, and 2D noise power spectra were calculated for each.

Visual examination of the noise power spectra did not suggest a useful metric for comparison of relative color uniformity, but they did reveal more complex behavioral differences that will be basis for follow up analysis.

Boxes—Another Spatial Domain Analysis

An $N \times N$ aperture box was defined where N is the number of virtual halftone dots.

The box was placed in the upper left hand corner of the virtual halftone, and additional boxes were placed in sequence to tile over the entire image.

Within each box the average reflectance spectrum and the corresponding $L^*a^*b^*$ value was found. Then the standard deviation for each color coordinate was calculated, σ_L , σ_a , and σ_b , and the overall RMS color deviation for the image was determined:

$$\sigma_E = (\sigma_L^2 + \sigma_a^2 + \sigma_b^2)^{1/2}$$

The value of N was then increased and the analysis repeated to generate



another value of σ_E . As anticipated, σ_E decreased as the aperture box size, N , increased.

We observed that σ_E increased linearly with $1/N$, and the following metrics of color variation were defined from these graphs. These three metrics of color variation are defined as follows, and their values for each of the 22 mask combinations are shown in Metrics Table.

Reading the Metrics Table

- (a) N_5 is the value of N for $\sigma_E = 5$. This corresponds to a color difference, σ_E , of 5, which is noticeable by most people but small. A value of 5 was used for comparison of the 22 mask combinations rather than the approximate JND of 1.0 because many of the mask combinations did not achieve $\sigma_E = 1$.
- (b) N_{min} is the value of N at which $\sigma_E = 0$. Several mask combinations did not show a zero color deviation even as the box size went to infinity ($1/N = 0$).
- (c) $\sigma_{E_{min}}$ is the value of σ_E at $1/N = 0$. This was included since even if a system did not have an N_{min} , it would always have a minimum σ_E .



Metrics Table for Cyan & Magenta Image Pairs

Image	Dist.	N_5	N_{min}	$\sigma_{E_{min}}$
$\langle G_0G_1 \rangle$	15	13.7	1042	0
$\langle G_0G_2 \rangle$	16	19.1	133	0.021
$\langle G_0G_3 \rangle$	16	14.0	∞	0.196
$\langle G_0G_4 \rangle$	16	13.9	∞	0.111
$\langle G_0G_5 \rangle$	17	17.1	102	0
$\langle G_0G_6 \rangle$	15	13.6	∞	0.017
$\langle G_0G_7 \rangle$	16	18.4	214	0.203
$\langle G_0T_0 \rangle$	15	19.0	70	0
$\langle G_0T_1 \rangle$	14	13.2	98	0
$\langle G_0T_2 \rangle$	14	18.9	113	0
$\langle G_0T_3 \rangle$	16	12.6	132	0

Image	Dist.	N_5	N_{min}	$\sigma_{E_{min}}$
$\langle G_0T_4 \rangle$	15	12.5	100	0
$\langle G_0T_5 \rangle$	14	19.0	84	0
$\langle G_0T_6 \rangle$	15	13.0	104	0
$\langle G_0T_7 \rangle$	15	18.9	131	0
$\langle T_0T_1 \rangle$	16	14.1	133	0
$\langle T_0T_2 \rangle$	15	18.0	103	0
$\langle T_0T_3 \rangle$	16	13.6	165	0
$\langle T_0T_4 \rangle$	16	13.4	251	0
$\langle T_0T_5 \rangle$	15	19.2	64	0
$\langle T_0T_6 \rangle$	16	14.0	177	0
$\langle T_0T_7 \rangle$	14	19.3	88	0

Observations & Conclusions

Examination of the four color uniformity metrics shows significant differences between the 22 mask combinations.

Contrary to our initial expectations, there was little correlation between the different metrics.

Further consideration suggests this should not be surprising.

Visual Distance Metric

The visual distance metric, Dist. , in column 2 varied only slightly among the 22 mask combinations, but the calculated metrics in columns 3, 4, and 5 varied much more.

The box metrics, N_5 and N_{min} were specifically designed to mimic the visual distance metric.

However, the spectrum of phosphors on the CRT monitor are quite different from the idealized spectra of the virtual halftones on which the box metrics are based.

In addition, the monitor resolution may tend to low-pass the simulated displayed halftone.



The overall effect is that visual inspection of a synthetic halftone on a monitor appears not to be a very sensitive index of relative color uniformity, at least as done in this project.

Further work is needed to develop a visual evaluation experiment to provide useful insights into the visual significance of color uniformity associated with different color halftone algorithms.

Box Metric

Among the three box metrics of color uniformity, the minimum color variation, σ_{min} , appears useful only as an index of the worst cases.

The most color uniform mask combinations all were capable of a zero color variation at some box size, N .

All of combinations with at least one of T_i type mask were capable of $\sigma_{min} = 0$, so further analysis was limited only to those 15 combinations.



Ideal Visual Distance

The N_5 and N_{min} metrics were intended to be a simulation of an ideal visual distance experiment.

In both cases, a smaller value indicates better color uniformity.

However, the correlation between these two metrics is very low, and indeed the correlation coefficient is negative ($r = -0.5$) for the 15 combinations containing a \mathcal{T} mask.

A plot of N_{min} vs. N_5 , below, shows the correlation.

The absence of a positive correlation, coupled with the apparent bimodal distribution suggests that a single color uniformity metric is insufficient to characterize the relative quality of spatial variations in color of the mask combinations.



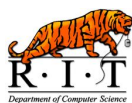
Work to be done

This work has not resulted in a clear preference for a single number metric for comparison of color uniformity of different types of halftone algorithms.

There may indeed be a single number metric, defined to correlate highly with appropriate visual preference experiments, but such a metric is clearly not a trivial matter to define.

Nor is it trivial to define an appropriate experimental protocol for visual assessment of color uniformity capabilities of halftone algorithms.

In particular, it is difficult to eliminate all artifacts associated with monitors.



This work does show, however, that different color halftone algorithms do result in significant differences in color uniformity.

Further work is being carried out develop better color halftone algorithms and to develop experimental protocols for their evaluation.

N_{min} vs. N_5 for Combination with at Least One \mathcal{T} Mask

